

## NGC 5385, NGC 2664 and Collinder 21: Three candidate open cluster remnants<sup>★,★★</sup>

S. Villanova<sup>1</sup>, G. Carraro<sup>1,2,3</sup>, R. de la Fuente Marcos<sup>4</sup>, and R. Stagni<sup>1</sup>

<sup>1</sup> Dipartimento di Astronomia, Università di Padova, Vicolo Osservatorio 2, 35122 Padova, Italy  
e-mail: villanova@pd.astro.it

<sup>2</sup> Departamento de Astronomía, Universidad de Chile, Casilla 36-D, Santiago, Chile

<sup>3</sup> Astronomy Department, Yale University, PO Box 208101, New Haven, CT 06520-8101, USA

<sup>4</sup> Suffolk University Madrid Campus, C/ Viña 3, 28003 Madrid, Spain

Received 20 April 2004 / Accepted 26 July 2004

**Abstract.** We present CCD *UBVI* photometric and medium/high resolution spectroscopic observations obtained in the field of the previously unstudied dissolving open cluster candidates NGC 5385, NGC 2664 and Collinder 21. Our analysis is based on the discussion of star counts, photometry, radial velocity distribution, and proper motions available from the Tycho 2 catalogue. All three aggregates clearly emerge from the mean Galactic field, but, regrettably, the close scrutiny of proper motions and radial velocities reveals that we are not facing any physical group. Instead, what we are looking at are just chance alignments of a few bright unrelated stars. Our analysis casts some doubt on the Bica et al. (2001, A&A, 366, 827) criterion to look for Possible Open Cluster Remnants. It seems mandatory to define a better criterion to adopt for further investigations.

**Key words.** Galaxy: open clusters and associations: individual: Collinder 21, NGC 5385, NGC 2664 – Galaxy: open clusters and associations: general – stars: binaries: close

### 1. Introduction

Bica et al. (2001) identified 34 neglected star clusters (see [http://obswww.unige.ch/webda/dissolving\\_ocl.html](http://obswww.unige.ch/webda/dissolving_ocl.html)) having relatively high galactic latitude ( $|b| > 15^\circ$ ), poorly populated and appearing to be candidate objects that are experiencing the late stages of star cluster dynamical evolution. For these objects the acronym POCR – Possible Open Cluster Remnant – is used. In their study, Bica et al. (2001) basically select these candidates on the basis of star counts. All of them indeed clearly emerge from the background.

The final residue of open star cluster evolution is often called an open cluster remnant (OCR). These ghostly objects are characterized by very low surface brightness and they are hardly distinguishable against the background field stars (de la Fuente Marcos 1998). They consist of a small number of coeval relatively massive stars, most of which are binaries, confined in a core, since due to the evolution the less massive star members have evaporated from the cluster and merged with the Galactic disk field (de la Fuente Marcos 1997).

Recently, these objects have started to receive some attention mainly because they play a fundamental role in our

understanding of the subject of open cluster evolution and dissolution, and, ultimately, of the origin of the field star population. Photometry, kinematics, binary percentage and membership are basic data to constrain *N*-body models of cluster dissolution, which aim to reconstruct – for instance – the Initial Mass Function (IMF) of Galactic clusters (e.g. de la Fuente Marcos 1997).

On the other hand, they may be what still remains of old clusters, and therefore once discovered they can allow us to improve the statistics of old open clusters in the Galactic disk. These objects are widely recognised to be of paramount importance for our understanding of the formation and early evolution of the Galactic disk (Carraro et al. 1998). Some POCR candidates have been studied recently.

The best discussed case is doubtless NGC 6994 (M 73), studied by Bassino et al. (2000), Carraro (2000) and Odenkirchen & Soubiran (2002). Combining photometry, astrometry and spectroscopy it was found that this object was just a chance alignment of four stars.

Pavani et al. (2001) discuss new photometry of NGC 1901 and NGC 1252, bringing new evidence that these stellar groups are POCRs. However, proper motion studies for NGC 1252 seem to point to the opposite conclusion (Baumgardt 1998). On the other hand, the radial velocity survey conducted by Villanova et al. (2003a,b) confirms that NGC 1901 is a genuine POCR.

\* Based on observations carried out at Mt Ekar Observatory, Asiago, Italy.

\*\* Photometry is only available in electronic form at the CDS via anonymous ftp to cdsarc.u-strasbg.fr (130.79.128.5) or via <http://cdsweb.u-strasbg.fr/cgi-bin/qcat?J/A+A/428/67>

**Table 1.** Basic parameters of the observed objects. Coordinates are for the J2000.0 equinox and have been taken from Dias et al. (2002).

Name	$\alpha$	$\delta$	$l$	$b$
	hh:mm:ss	° : ' : "	°	°
NGC 5385	13:52:27	+76:10:24	118.19	+40.38
NGC 2664	08:47:11	+12:36:06	214.34	+31.31
Collinder 21	01:50:11	+27:04:00	138.73	-33.99

Finally, on the basis of only star counts and photometry, Carraro (2002) discusses the cases of NGC 7772 and NGC 7036 and Baume et al. (2003) that of NGC 1663; they favor the possibility that these two objects are indeed OCRs and provide a list of possible candidate members for spectroscopic follow up.

In this paper we present a photometric, astrometric and spectroscopic investigation of three previously unstudied POCs, namely NGC 5385, NGC 2664, and Collinder 21, with the aim of clarifying their real nature. The analysis closely follows the strategy earlier proposed by Odenkirchen & Soubiran (2002).

The layout of this paper is as follows.

In Sect. 2 we briefly present the observations and data reduction. Section 3 illustrates star count analysis and spatial configurations. Section 4 is dedicated to the results of the proper motion analysis, and in Sect. 5 we discuss our spectroscopy. Our conclusions are presented in Sect. 6.

## 2. Observations and data reduction

### 2.1. Photometry

Observations were carried out with the AFOSC camera at the 1.82 m Copernico telescope of Cima Ekar (Asiago, Italy), in the photometric nights of December 17 and 18, 2001. AFOSC samples a  $8'14 \times 8'14$  field on a  $1K \times 1K$  thinned CCD. The typical seeing was between 1.8 and 2.3 arcsec. The basic data of the studied objects are summarized in Table 1, and the details of the observations are listed in Table 2.

The data have been reduced using the IRAF<sup>1</sup> packages CCDRED, DAOPHOT, and PHOTCAL. The calibration equations obtained by observing Landolt (1992) SA 93, PG 1047+003, PG 2331+055 and PG 0231+051 fields during both nights are:

$$\begin{aligned}
 u &= U + 3.520 \pm 0.042 + (0.099 \pm 0.030)(U - B) + 0.58 X \\
 b &= B + 1.407 \pm 0.012 - (0.004 \pm 0.017)(B - V) + 0.29 X \\
 v &= V + 0.752 \pm 0.009 + (0.036 \pm 0.012)(B - V) + 0.16 X \\
 i &= I + 1.619 \pm 0.017 - (0.011 \pm 0.015)(V - I) + 0.08 X \quad (1)
 \end{aligned}$$

where  $UBVI$  are standard magnitudes,  $ubvi$  are the instrumental ones, and  $X$  is the airmass. The standard stars in these fields provide a very good color coverage,

<sup>1</sup> IRAF is distributed by the National Optical Astronomy Observatories, which are operated by the Association of Universities for Research in Astronomy, Inc., under cooperative agreement with the National Science Foundation.

**Table 2.** Journal of photometric observations in the field of Collinder 21, NGC 5385, and NGC 2664 and standard star fields (December 17–18, 2001).

Field	Filter	Time integration (s)	Seeing (")
Collinder 21	<i>U</i>	15, 60	2.1
	<i>B</i>	2, 5, 15	2.0
	<i>V</i>	1, 3, 10, 10	2.1
	<i>I</i>	1, 8	2.0
SA 93	<i>U</i>	120	1.9
	<i>B</i>	60, 60	2.0
	<i>V</i>	30, 30, 30	2.0
	<i>I</i>	30, 30	2.0
NGC 5385	<i>U</i>	240	2.2
	<i>B</i>	60, 60	2.1
	<i>V</i>	15, 15	2.3
	<i>I</i>	15, 15	2.3
PG 1047+003	<i>U</i>	120	1.9
	<i>B</i>	60, 60	2.0
	<i>V</i>	30, 30	2.0
	<i>I</i>	30, 30	2.0
PG 0231+051	<i>U</i>	120	1.9
	<i>B</i>	60, 60	2.0
	<i>V</i>	30, 30	2.0
	<i>I</i>	30, 30	2.0
PG 2331+055	<i>U</i>	120	1.9
	<i>B</i>	60, 60	2.0
	<i>V</i>	30, 30	2.0
	<i>I</i>	30, 30	2.1
NGC 2664	<i>U</i>	15, 240	1.8
	<i>B</i>	1, 10, 60	1.7
	<i>V</i>	1, 5, 30, 30	1.8
	<i>I</i>	1, 5, 30	1.8

viz.  $-0.329 \leq (B - V) \leq 1.448$ . For the extinction coefficients we assumed the typical values for the Asiago Observatory (Desidera et al. 2001). Photometric global errors have been estimated following Patat & Carraro (2001). For the *V* filter, they amount to 0.02, 0.04 and 0.08 at  $V \approx 12.0$ , 16.0 and 20.0, respectively.

The photometry for the most obvious candidates is reported in Tables 3 to 5; all the photometric catalogues are available upon request to the authors.

### 2.2. Spectroscopy

Medium ( $R \approx 3600$ ) and high resolution ( $R \approx 20000$ ) spectra in the field of NGC 5385, NGC 2664 and Collinder 21 have been obtained using AFOSC in Echelle mode (in the grism #9

**Table 3.** Photometry and proper motion of the most obvious candidate members in the field of NGC 5385.

ID	TYC 4558-	$\alpha(J2000.0)$	$\delta(J2000.0)$	$V$	$(B - V)$	$(U - B)$	$\mu_\alpha \cos \delta$ [mas/yr]	$\mu_\delta$ [mas/yr]
1	1641	13:52:54.104	+76:09:59.63	11.29	0.50	0.18	$-7.5 \pm 1.9$	$11.7 \pm 2.1$
2	1385	13:52:08.976	+76:10:55.12	11.52	0.39	0.14	$2.5 \pm 2.0$	$-3.0 \pm 2.1$
3	457	13:51:58.757	+76:13:20.41	11.39	0.58	0.32	$-44.6 \pm 2.0$	$-6.6 \pm 2.1$
4	399	13:52:18.535	+76:10:45.58	11.31	0.68	0.39	$-29.0 \pm 2.3$	$13.8 \pm 2.3$
5	1797	13:51:49.975	+76:12:11.67	11.32	0.72	0.56	$-23.6 \pm 2.1$	$17.0 \pm 2.2$
6	1873	13:52:32.078	+76:08:07.41	11.78	0.64	0.33	$-42.2 \pm 2.2$	$26.8 \pm 2.3$
7	217	13:52:34.850	+76:11:10.84	11.77	1.04	1.03	$-12.5 \pm 2.3$	$6.5 \pm 2.4$

**Table 4.** Photometry and proper motion of the most obvious candidate members in the field of NGC 2664.

ID	TYC 816-	Name	$\alpha(J2000.0)$	$\delta(J2000.0)$	$V$	$(B - V)$	$(U - B)$	$(V - I)$	$\mu_\alpha \cos \delta$ [mas/yr]	$\mu_\delta$ [mas/yr]
1	2354	BD+13 1898	08:47:11.173	+12:37:58.63	10.75	0.43	0.19	0.69	$-6.4 \pm 1.9$	$5.6 \pm 2.1$
2	1826		08:46:58.629	+12:37:10.47	11.11	0.37	0.29	0.61	$-8.3 \pm 2.0$	$-4.7 \pm 2.1$
3	1890		08:47:13.795	+12:36:13.50	10.99	1.03	1.05	1.13	$1.5 \pm 2.0$	$-26.0 \pm 2.1$
4	2400	BD+13 1899	08:47:06.699	+12:34:38.76	11.41	1.11	0.99	1.15	$-2.6 \pm 2.3$	$3.2 \pm 2.3$

**Table 5.** Photometry and proper motion of the most obvious candidate members in the field of Collinder 21.

ID	TYC 1759-	Name	$\alpha(J2000.0)$	$\delta(J2000.0)$	$V$	$(B - V)$	$(U - B)$	$(V - I)$	$\mu_\alpha \cos \delta$ [mas/yr]	$\mu_\delta$ [mas/yr]
1	450	BD+26 307	01:50:11.56	+27:01:59.0	8.20	0.45			$56.5 \pm 1.5$	$-33.5 \pm 0.9$
2	1472	BD+26 304	01:50:01.41	+27:03:40.0	9.80	0.61		0.82	$5.1 \pm 1.2$	$-11.0 \pm 1.2$
3	1025	BD+26 306	01:50:12.17	+27:07:47.1	9.69	1.75	1.65		$-8.7 \pm 1.4$	$-1.1 \pm 1.4$
4	468		01:50:08.22	+27:07:00.2	11.32	1.39	1.50	1.46	$-0.7 \pm 2.3$	$-3.3 \pm 2.3$
5	994		01:50:13.40	+27:05:57.5	11.17	0.74	0.44	0.95	$48.7 \pm 1.9$	$-11.5 \pm 1.9$
6	462		01:50:27.06	+27:04:09.7	11.32	0.59	0.26	0.83	$-6.4 \pm 1.9$	$-8.4 \pm 1.9$
7	1333		01:50:08.53	+27:01:49.4	11.61	0.89	0.69	1.07	$-6.9 \pm 1.2$	$+16.7 \pm 0.9$
8	266		01:50:05.23	+27:02:00.0	11.21	0.98	0.79	1.14	$24.1 \pm 1.9$	$4.3 \pm 1.9$
9	866	BD+26 305b	01:50:02.41	+27:06:13.8	10.09	0.85	0.58	1.04	$-3.9 \pm 1.3$	$-6.7 \pm 1.2$
10	1114	BD+26 305a	01:50:02.08	+27:05:56.6	10.36	1.08	1.08	1.18	$-3.6 \pm 1.8$	$-5.0 \pm 1.8$
11	1749		01:50:18.14	+27:04:28.9	12.34	0.56	0.27	0.78	$11.9 \pm 2.3$	$-5.5 \pm 2.3$
12	272		01:50:23.97	+27:02:23.1	12.81	0.65	0.27	0.86	$1.9 \pm 1.3$	$-8.4 \pm 2.9$

Note: star #1 was saturated in our photometry, and magnitude and color have been taken from Tycho-2. Stars #7 and #12 have been taken from the UCAC2 catalog.

and #10 combination) and the REOSC Echelle Spectrograph onboard the 1.82 m telescope of Asiago Astronomical Observatory.

The Echelle spectrograph works with a Thomson 1024 × 1024 CCD and the allowed wavelength coverage is approximately 4140–6840 Å. Details on this instrument are given in Munari & Zwitter (1994) and on the Asiago Observatory Home page<sup>2</sup>.

The exposures times were 45 min for all stars. To improve the signal to noise ratio two exposures were taken for each star reaching  $S/N$  values up to 150. The data were reduced with the IRAF package ECHELLE using thorium lamp spectra for wavelength calibration purposes. By comparing known sky lines positions along the spectra we obtained an error measurement of about 0.01 Å.

The AFOSC spectra cover the wavelength range 4100–6800 Å, and for typical exposure times of 30 to

60 min we obtained  $S/N$  values up to 300, which allows us to derive radial velocities with errors almost always lower than  $8 \text{ km s}^{-1}$ . In this case, the data were reduced with the IRAF package for one-dimensional spectroscopy *CTIOSLIT* and using the Hg-Cd lamp spectra for wavelength calibration purposes. Together with radial velocities we also provide spectral classifications, which were derived as described in Villanova et al. (2004).

In Tables 6 to 8 we report some details of the spectroscopic observations.

### 3. Star counts, surface density and spatial distribution

POCRs are identified by Bica et al. (2001) as star overdensities at relatively high galactic latitudes. For star count purposes we have used USNO-B1 (Monet et al. 2003) catalogue for NGC 5385 and UCAC2 (Zacharias et al. 2003) catalogue for NGC 2664 and Collinder 21, because UCAC2 does not

<sup>2</sup> <http://www.pd.astro.it/Asiago/2000/2300/2320.html>

**Table 6.** Spectroscopic results for NGC 5385.

ID	TYC 4558-	Date of observation	<i>S/N</i>	Resolution	Julian date	Rad. vel [km s <sup>-1</sup> ]	Sp. type	[Fe/H] [dex]	( <i>m</i> - <i>M</i> ) <sub>V</sub> [mag]
1	1641	12/07/2002	120	20 000	2 452 467.4011	-10.5 ± 1.2	F6 V	+0.2 ± 0.3	7.49
		15/02/2003		20 000	2 452 685.6788	-7.5 ± 1.0			
		12/05/2003		20 000	2 452 772.3750	-6.9 ± 0.3			
2	1385	12/07/2002	110	20 000	2 452 468.3527	-61.8 ± 2.3	F4 V	+0.4 ± 0.3	8.07
		15/02/2003		20 000	2 452 685.5271	-62.5 ± 1.0			
		12/05/2003		20 000	2 452 772.4526	-62.4 ± 0.3			
3	457	12/07/2002	120	20 000	2 452 468.4014	-1.9 ± 1.3	F8 V	+0.9 ± 0.4	7.19
		15/02/2003		20 000	2 452 685.6436	-1.1 ± 1.0			
		12/05/2003		20 000	2 452 772.5267	-1.5 ± 0.3			
4	399	12/07/2002	120	20 000	2 452 467.4495	2.5 ± 1.8	G2 V	+0.4 ± 0.3	6.51
		15/02/2003		20 000	2 452 685.5377	1.1 ± 1.0			
		12/05/2003		20 000	2 452 772.4272	4.9 ± 0.3			
5	1797	12/07/2002	120	20 000	2 452 468.4493	-12.0 ± 0.7	G6 IV	+0.3 ± 0.3	8.17
		15/02/2003		20 000	2 452 685.6092	-11.3 ± 1.0			
		12/05/2003		20 000	2 452 772.5043	-12.3 ± 0.3			
6	1873	12/07/2002	90	20 000	2 452 469.4313	38.1 ± 0.7	G1 V	+0.5 ± 0.4	7.08
		15/02/2003		20 000	2 452 685.7243	29.4 ± 1.0			
		12/05/2003		20 000	2 452 772.4789	28.7 ± 0.3			
7	217	12/07/2002	90	20 000	2 452 469.3571	3.8 ± 0.7	K4 V	+0.3 ± 0.3	4.87
		15/02/2003		20 000	2 452 685.4985	4.0 ± 1.0			
		12/05/2003		20 000	2 452 772.4015	3.7 ± 0.2			

**Table 7.** Spectroscopic results for NGC 2664.

ID	TYC 816-	Date of observation	<i>S/N</i>	Resolution	Julian date	Rad. vel [km s <sup>-1</sup> ]	Sp. type	[Fe/H] [dex]	( <i>m</i> - <i>M</i> ) <sub>V</sub> [mag]
1	2354	15/01/2003	160	20 000	2 452 655.5065	26.0 ± 2.0	F5 IV-V	+0.3 ± 0.3	7.70
		12/05/2003		20 000	2 452 772.3168	27.1 ± 0.3			
2	1826	15/01/2003	130	20 000	2 452 656.4174	13.5 ± 1.5			
		06/12/2003		20 000	2 452 979.5724	54.4 ± 3.5			
3	1890	15/01/2003	140	20 000	2 452 655.5844	14.4 ± 1.5	K0 III	+0.6 ± 0.4	9.79
		12/05/2003		20 000	2 452 772.3446	12.7 ± 0.3			
4	2400	15/01/2003	110	20 000	2 452 656.5643	23.0 ± 1.5	K1 III	+0.1 ± 0.3	10.41
		06/12/2003		3600	2 452 979.6014	20.5 ± 4.1			

extend to the declination of NGC 5385. In the following we will compare star counts inside the OCR region with star counts in an off-set field, which is chosen to represent the mean Galactic disk field.

A crucial role in star counts is played by binaries. Anticipating the results of Sect. 5 we find that in the OCRs under investigation the binary fraction ranges from 18% to 25%, a value which is not very different from the estimated typical percentage in the Galactic disk field population, which in the proper *F* - *K* spectral range amounts to about 14% (Halbwachs et al. 2003). If one also considers *M* type stars, this percentage would increase.

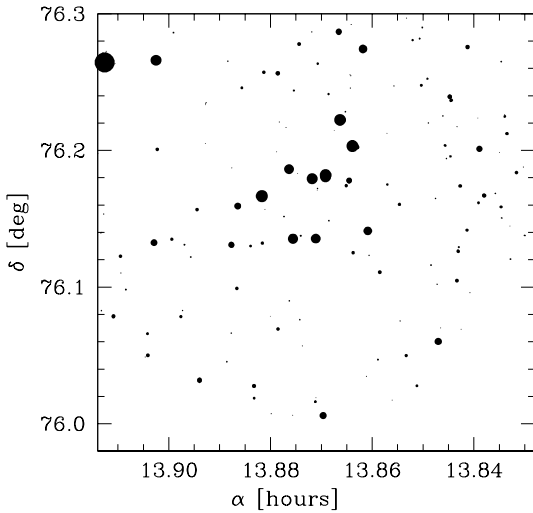
Therefore we do not expect that binary stars significantly affect the star counts.

### 3.1. NGC 5385

Figure 1 shows a finding chart in a 20' × 20' region around NGC 5385 down to *B* = 21.5 according to USNO-B1. The center of this image, which we also consider the center of NGC 5385, has been derived as the mean of the position of the 9 most obvious members of the aggregate. Indeed this object seems to consist of 9 stars with magnitudes 11 ≤ *B* ≤ 13 in a field of about 3'5 × 3'5. The aggregate appears rather

**Table 8.** Spectroscopic results for Collinder 21.

ID	TYC 1759-	Date of observation	$S/N$	Resolution	Julian date	Rad. vel [ $\text{km s}^{-1}$ ]	Sp. type	$(m - M)_V$ [mag]
1	450	04/07/2002	530	20 000	2 452 468.5756	$-3.2 \pm 0.7$	F9 V	3.90
		20/09/2003	300	3600	2 452 902.5724	$7.4 \pm 5.5$		
		05/12/2003		3600	2 452 979.1951	$42.4 \pm 4.8$		
2	1472	20/09/2003	360	3600	2 452 902.5906	$5.3 \pm 6.2$	G0 V	5.35
		05/12/2003		3600	2 452 979.2083	$11.7 \pm 5.7$		
3	1025	20/09/2003	330	3600	2 452 902.6222	$55.2 \pm 7.8$	M8 III	10.84
		05/12/2003		3600	2 452 979.4393	$68.3 \pm 11.4$		
4	468	09/10/2003	210	3600	2 452 922.4483	$-25.5 \pm 4.4$	K2 III	10.52
		05/12/2003		3600	2 452 979.2983	$-15.9 \pm 10.3$		
5	994	09/10/2003	230	3600	2 452 922.4725	$46.9 \pm 7.3$	G8 V	5.67
		05/12/2003		3600	2 452 979.2378	$37.5 \pm 8.0$		
6	462	09/10/2003	210	3600	2 452 922.5142	$42.9 \pm 7.4$	G3 V	6.32
		05/12/2003		3600	2 452 979.3997	$24.8 \pm 6.4$		
7	1333	05/12/2003	190	3600	2 452 979.5238	$48.5 \pm 4.6$	K2 V	5.31
		04/01/2004		3600	2 453 009.3715	$57.0 \pm 5.2$		
8	266	20/09/2003	230	3600	2 452 902.4968	$50.7 \pm 4.6$	G8 III	9.86
		04/01/2004		3600	2 453 009.3979	$40.4 \pm 5.2$		
9	866	20/09/2003	310	3600	2 452 902.4559	$3.5 \pm 5.7$	G5 III	9.49
		04/01/2004		3600	2 453 009.4311	$17.2 \pm 7.9$		
10	1114	20/09/2003	270	3600	2 452 902.5238	$48.5 \pm 4.6$	K1 III	9.36
		04/01/2004		3600	2 453 010.3701	$5.2 \pm 5.7$		
11	1749	20/09/2003	150	3600	2 452 980.2946	$24.8 \pm 7.2$	F8 V	8.14
		04/01/2004		3600	2 453 010.3303	$23.0 \pm 7.1$		
12	272	20/09/2003	120	3600	2 452 980.3317	$33.9 \pm 7.3$	G0 V	8.36
		04/01/2004		3600	2 453 010.2885	$41.2 \pm 8.3$		

**Fig. 1.** Distribution of stars from the USNO-B1 catalogue in a  $20' \times 20'$  field around NGC 5385. The sizes of the dots are proportional to the magnitudes of the stars.

sparse; the mean mutual angular separation is larger than  $30''$ . Outside of the central group there is a clear deficiency of stars with similar brightnesses, which appear at least 1 mag

fainter on the average, except for some obvious stars north of NGC 5385.

In Fig. 2 we show the surface density of stars of different magnitudes as a function of angular distance from the center of NGC 5385, (based on USNO-B1). The central group of bright stars produces a significant local enhancement in the surface density of stars with magnitudes  $B \leq 13.5$  (see panel (a)). Fainter stars in the magnitude bins  $13.5 \leq B \leq 17.0$  (panel (b))  $B \geq 18.0$  (panel (c)) do not show any signs of a spatial concentration; star counts in the cluster area always agree within the uncertainties with those in the off-set field. In fact in the lower panel the overdensity in the central part is too close to the noise level to be considered significant.

In conclusion only the brightest stars indicate the existence of a cluster, and we looked for membership in this magnitude range. This of course does not exclude that fainter stars could also be members, if the cluster turns out to be a physical one.

### 3.2. NGC 2664

Figure 3 shows the distribution of stars in a field of  $30' \times 30'$  around NGC 2664 down to a magnitude UCmag (between  $V$  and  $R$ ) of  $\approx 16.3$  according to UCAC2. This figure reveals that NGC 2664 is defined by 4 stars with magnitude

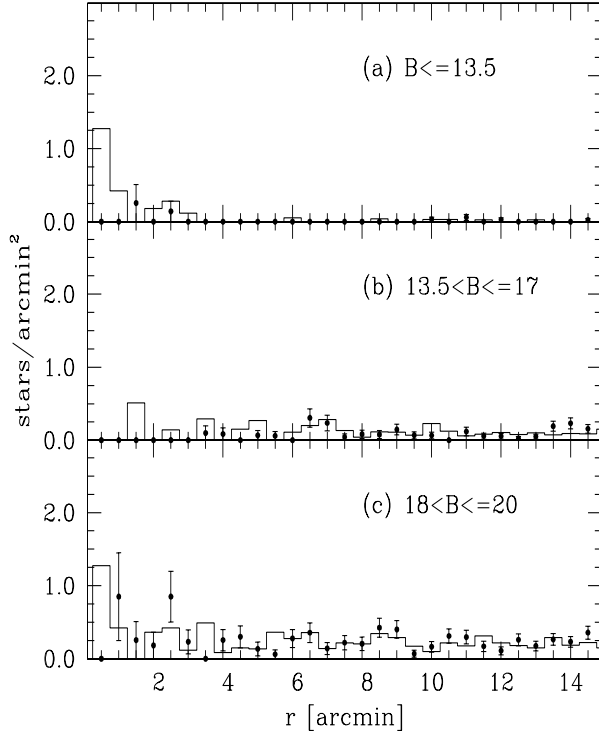


**Fig. 2.** Histogram of the surface density of the stars shown in Fig. 1, measured by counts in 0.5 wide annuli centered on  $\alpha = 13^{\text{h}}52^{\text{m}}19^{\text{s}}$ ,  $\delta = +76^{\circ}10'56''$ . Dots with error bars indicate the mean surface density of stars in a nearby field centered on  $\alpha = 13^{\text{h}}54^{\text{m}}10^{\text{s}}$ ,  $\delta = +76^{\circ}49'30''$ , and the expected  $1\sigma$  range of statistical fluctuations around this mean for each bin.

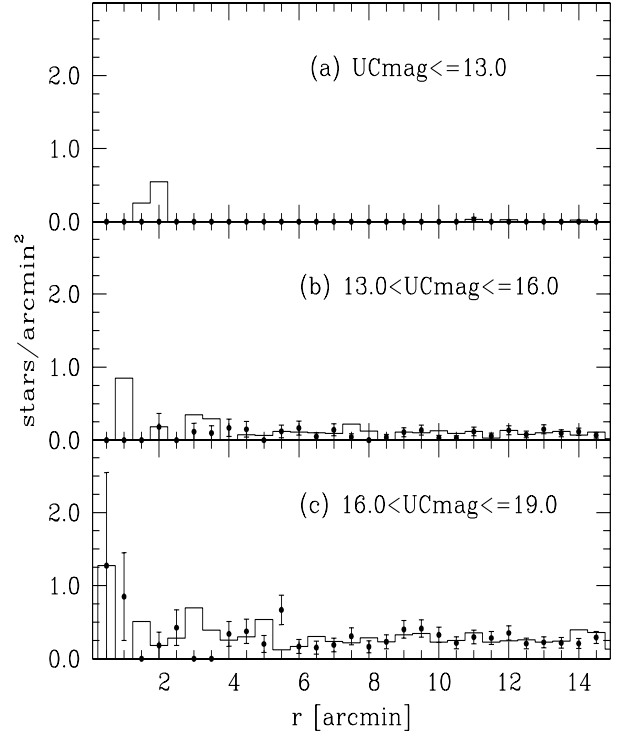


**Fig. 4.** Histogram of the surface densities of the stars shown in Fig. 3, measured by counts in 0.5 wide annuli centered on  $\alpha = 08^{\text{h}}47^{\text{m}}07^{\text{s}}$ ,  $\delta = +12^{\circ}36'30''$ . Dots with error bars indicate the mean surface density of stars in a nearby field centered on  $\alpha = 08^{\text{h}}53^{\text{m}}05^{\text{s}}$ ,  $\delta = +12^{\circ}59'50''$ , and the expected  $1\sigma$  range of statistical fluctuations around this mean for each bin.

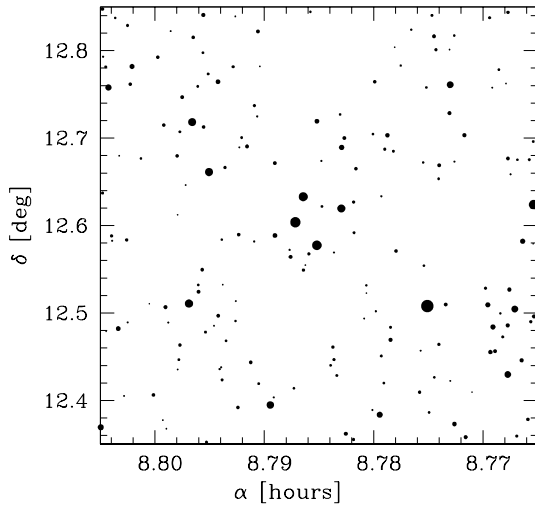


**Fig. 3.** Distribution of stars from the UCAC2 catalogue in a  $30' \times 30'$  field around NGC 2664. The sizes of the dots are proportional to the magnitudes of the stars.

$10.5 \leq UCmag \leq 11.5$  confined within  $2.5 \times 2.5$  arcmin around the nominal center, taken as the mean of the positions of the four most obvious members. In the immediate surroundings there is a clear lack of bright stars, although about  $3'$  from the cluster center the field is quite rich in bright stars, and a few other concentrations of the same kind as NGC 2664 seem to be present.

In Fig. 4 we show the surface density of stars of different magnitudes as a function of angular distance from the center of NGC 2664, (also based on UCAC2). The central group of bright stars produces a small but sizeable local enhancement in the surface density of stars with magnitudes  $UCmag \leq 13.5$  (see panel (a)). The same seems to occur for the magnitude bins  $13.0 \leq UCmag \leq 16.0$  (panel (b)), whereas fainter stars, in the magnitude bin  $UCmag \geq 16.0$  (panel (c)) do not show any clear sign of a spatial concentration. At all distances the cluster density profile is comparable with the field, except at a distance of 3 arcmin where there seems to be significant enhancement.

Therefore, the asterism NGC 2664 seems to be mainly identified by four bright stars and a few fainter stars in its immediate vicinity.

### 3.3. Collinder 21

Figure 5 shows the distribution of stars in a field of  $30' \times 30'$  around Collinder 21 down to a magnitude of  $\approx 15.3$  according to UCAC2. The appearance of Collinder 21 (also designated as OCL 371 and C0147+270) on the sky is very impressive. It consists of about 10 stars distributed in a ring-like structure in a very poorly populated field, which makes this structure emerge very sharply. There are two well known binary stars in this circlet: the visual binary system BD+26 305AB and the binary HD 11142, resolved by speckle interferometry, which

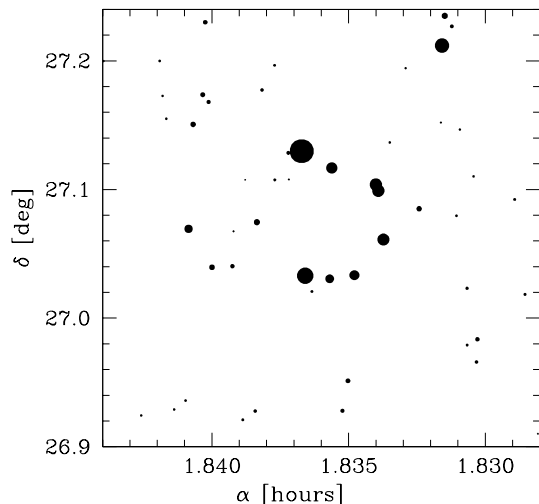


**Fig. 5.** Distribution of stars from the UCAC2 catalogue in a  $30' \times 30'$  field around Collinder 21. The sizes of the dots are proportional to the magnitudes of the stars.

presents a separation of  $0''.56$  between its components. All the other stars have much larger angular separation.

In Fig. 6 we show the surface densities of stars of different magnitudes as a function of angular distance from the center of Collinder 21, based on USNO-B1. The bright stars belonging to the circlet produce a significant local enhancement in the surface density of stars with magnitudes  $UCmag \leq 13.0$  (see panel (a)) at a distance corresponding to the radius of the circlet. Fainter stars in the magnitude bins  $13.0 \leq UCmag \leq 16.0$  (panel (b))  $UCmag \geq 16.0$  (panel (c)) do not show any signs of a spatial concentration since star counts in the cluster area always agree within the uncertainties with the nearby fields ones.

The only exception is again at a distance of about 3 arcmin, where the enhancement is significant at the  $2\sigma$  level. In conclusion star counts suggests that a clear concentration exist in the region of Collinder 21.

We would like to stress that the existence of some star over-density is a necessary condition for a physical cluster to exist, but not a sufficient one. We repeat here the analysis proposed by Odenkirchen & Soubiran (2002), to show what the actual number statistics can tell us about these three objects.

We use their Eq. (1):

$$p(n) = \frac{1}{n!} (\Sigma\pi\Theta^2)^n \exp(-\Sigma\pi\Theta^2) \quad (2)$$

which gives us the probability of finding  $n$  neighbours in a circular field of radius  $\Theta$  around an arbitrarily selected star, for a random distribution of stars with mean surface density  $\Sigma$ .

The statistics of star counts in the comparison fields for NGC 5385, NGC 2664 and Collinder 21 provide a mean surface density of 20, 16 and 64 stars/deg<sup>2</sup>, respectively, in the magnitude range  $10.0 \leq mag \leq 13.0$ .

In the case of NGC 2664, we investigate the probability of finding three or more neighbours within a radius of 2.5 arcmin. This turns out to be lower than  $1.2 \times 10^{-4}$ . For NGC 5385 we must look for the probability to find at least 8 neighbours within about 3 arcmin; this probability amounts to less than  $1.1 \times 10^{-11}$ . Finally, in the case of Collinder 21, we need at

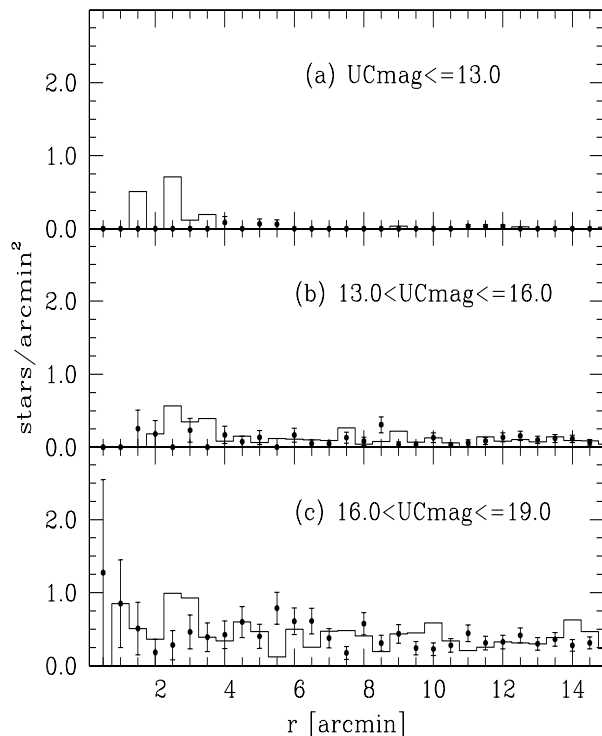


**Fig. 6.** Histogram of the surface densities of the stars shown in Fig. 5, measured by counts in  $0.5'$  wide annuli centered on  $\alpha = 01^{\text{h}}50^{\text{m}}11^{\text{s}}$ ,  $\delta = +27^{\circ}04'26''$ . Dots with error bars indicate the mean surface density of stars in a nearby field centered on  $\alpha = 01^{\text{h}}54^{\text{m}}10^{\text{s}}$ ,  $\delta = +27^{\circ}44'00''$ , and the expected  $1\sigma$  range of statistical fluctuations around this mean for each bin.

least 5 neighbours within about 3 arcmin, and the corresponding probability turns out to be less than  $4.4 \times 10^{-4}$ .

These numbers tell us that random configurations like those we are facing are rare. As a consequence, in all three cases (and especially for NGC 5385) we cannot exclude that these are physical groupings, and therefore only proper motions and radial velocities can settle the question of their real nature.

#### 4. Proper motion analysis

Important information on the kinematics of the luminous stars in and around our targets can be derived from the proper motions available in the Tycho-2 catalogue (Høg et al. 2000). We decided to opt for this catalogue because it provides homogeneous proper motion data for all the targeted stars. The recently released UCAC2 catalogue does not provide data for Collinder 21.

In Figs. 7, 9 and 11 we show the finding charts of our targets, in a field which corresponds roughly to our photometric survey, and indicate the stars for which we have proper motion measurements at our disposal. Moreover, Tables 3 to 5 list proper motion values, magnitudes and colors for the most obvious candidate members of the aggregates under investigation.

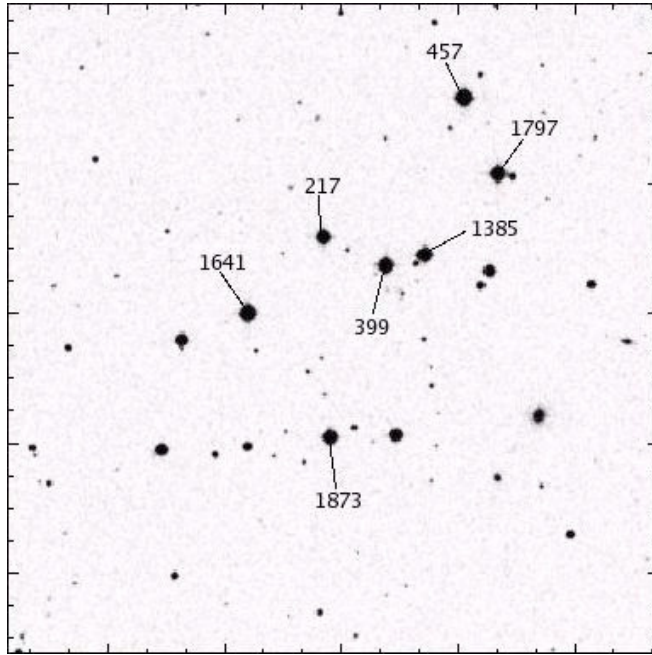


**Fig. 7.** Identification map ( $8'14 \times 8'14$ ), taken from DSS-2) for member candidates of NGC 5385 for which there are proper motions measurements from Tycho 2. North is up, East on the left. The labels give the star numbers assigned in the Tycho-2 catalog (in the sense TYC 4558- < ... >). The data for these stars are given in Tables 3 and 6.

#### 4.1. NGC 5385

The vector point diagram for all the candidate member stars having proper motion measurements in the field of NGC 5385 (see Fig. 7 for their identification) from the Tycho 2 catalogue is shown in Fig. 8, where panel a) present the Color–Magnitude Diagram (CMD) derived from our photometry, and panel b) shows the proper motion distribution. Of the 10 brightest stars that presumably define the aggregate (they are clearly detached from the bulk of the stars), 7 are plotted with open squares, and these are the stars for which we obtained a radial velocity measurement (see below). However, in the Tycho 2 catalogue we found proper motion for all 10 stars, and the three for which no radial velocity measurement is available are plotted with filled triangles. The remaining stars are plotted as open circles.

It is evident that these stars do not share a common mean tangential motion. In fact individual proper motion vectors range from about 5 to 63  $\text{mas yr}^{-1}$ , while the typical uncertainty of the proper motions is about 2  $\text{mas yr}^{-1}$  per component. This spread in tangential motion is seen to be in agreement with that shown by field stars in the surroundings of NGC 5385. We therefore suggest that the stars belonging to NGC 5385 simply are part of the local Galactic field.

#### 4.2. NGC 2664

The vector point diagram for all the candidate member stars in the field of NGC 2664 (see Fig. 9 for the identification) for which there are proper motion measurements from the Tycho-2 catalogue is shown in Fig. 10, together with the CMD obtained

from our photometry. Also in this case, there is a group of stars sharply detached from the bulk of the stars in the field. There are four of these, and they are plotted as squares in both panels.

It is evident that these stars do not share a common mean tangential motion. In fact individual proper motion vectors range from about 4 to 26  $\text{mas yr}^{-1}$ , while the typical uncertainty of the proper motions is about 2  $\text{mas yr}^{-1}$  per component. However, we note that stars #2354 and #2400 have a quite similar (within the errors) tangential motion, and might constitute a physical pair. The spread in tangential motion is also seen in this case to be in agreement with that shown by field stars in the surroundings of NGC 2664.

#### 4.3. Collinder 21

The CMD and the vector point diagram for all the candidate member stars (see Fig. 11 for the identification) for which there are proper motion measurements in the field of Collinder 21 from the Tycho-2 catalogue are shown in Fig. 12. 12 bright stars, in the magnitude range  $8 \leq V \leq 13$ , define the aggregate and are plotted in both panels as open squares. Proper motions are also available for three dimmer stars (solid triangles) which form a bridge (see the CMD in panel a)) from the brightest group to the bulk of the stars in the field. However these 3 stars have significantly diverse proper motion components (see Table 5). Coming back to the 12 brightest stars, their proper motion vectors range from about 3 to 68  $\text{mas yr}^{-1}$ , while the typical uncertainty of the proper motions is about 2  $\text{mas yr}^{-1}$  per component. It is evident that these stars do not share a common mean tangential motion. There are two clear pairs. One is the well known visual binary system BD+26 305ab (stars #866 and #1114), and the other is composed of the stars #1472 and #272, which deserve further investigation. Apart from these two pairs, the bulk of the stars exhibits a random motion.

### 5. Spectroscopic analysis

Multi-epoch spectra have been acquired for all the candidate members (23 stars in total for a grand total of 54 spectra) in the aggregates under investigations. The results of the spectroscopic survey are listed in Tables 6 to 8.

#### 5.1. NGC 5385

For this object we provide three epochs of Echelle spectra for seven bright stars, which all turn out to be dwarfs (see Table 6), except for star #1797, which seems to be a subgiant. Looking at the results in this table we find that two stars are probably unresolved binary stars (#1641 and #1873), whereas all the other stars do not exhibit significant variations in their radial velocity. The studied stars have radial velocities ranging from  $-62 \text{ km s}^{-1}$  to  $+30 \text{ km s}^{-1}$ , suggesting that NGC 5385 is not a physical aggregate. There might be some common motion pairs in this sample. Stars #399 and #1797 (see Table 3) have marginally consistent proper motion components, as have stars #1641 and #217. The first couple also has compatible spectral type (see Table 6). However, the radial velocities (see



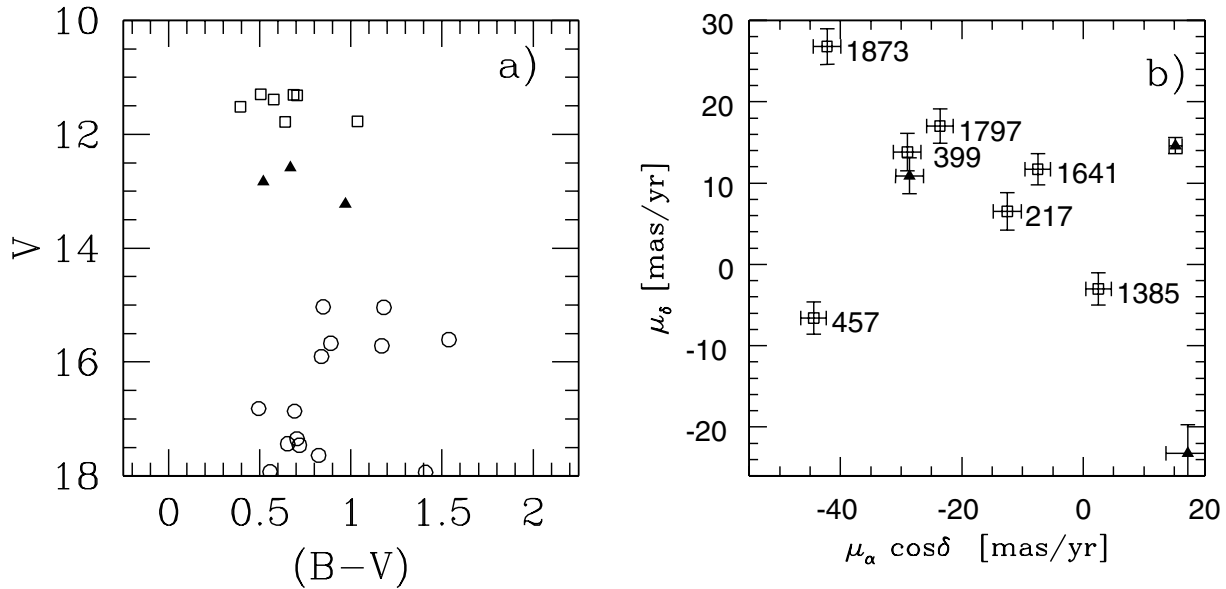


**Fig. 8.** Photometry and proper motions in the region of NGC 5385. **a)** Color–magnitude diagram. Open squares are Tycho 2 stars for which there are both proper motion and radial velocity measurements (see panel b) and Table 6), while filled triangles are stars having only proper motion measurements. **b)** Vector point plot of Tycho 2 proper motions and proper motion errors. Symbols are as in panel a). The identification numbers are from Tycho 2. See text for more details.

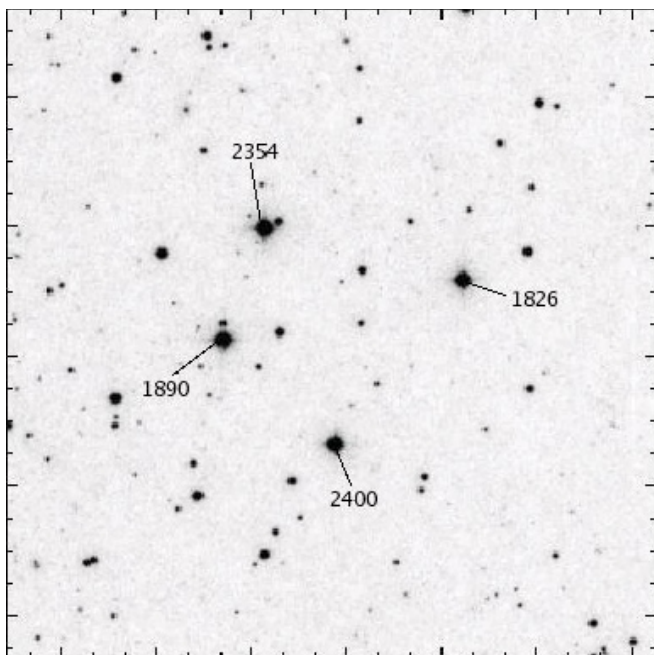


**Fig. 9.** Identification map ( $8'.14 \times 8'.14$ , taken from DSS-2) for member candidates of NGC 2664 for which there are proper motions measurements from Tycho 2. North is up, East on the left. The labels give the star numbers assigned in the Tycho-2 catalog (in the sense TYC 816– < ... >). The data for these stars are given in Tables 4 and 7.

Table 6) contradict this hypothesis. Moreover the pair members are located in very different positions (see Fig. 7).

We derived stellar distances from the Sun based on the spectral classification reported in Table 6. The relation between spectral type, luminosity class and absolute magnitude

was taken from the Michigan Spectral Catalogue Project<sup>3</sup>. The distance moduli range from 4.87 to 8.17 mag, which turn into distances of 94 to 430 pc. The extinction maps of Schlegel et al. (1998) provide a reddening of 0.04 mag for NGC 5385 region, which does not significantly alter the derived distances. The significant spread of distances rules out the possibility they form a physical group.

Metal abundances were derived using the MOOG code (freely distributed by Chris Sneden, University of Texas, Austin) as described in Carraro et al. (2004). The  $S/N$  ratio and the limited resolution prevented us from deriving very precise metallicity estimates, and therefore the value reported in Table 6 must be taken as an indication. We find that within the uncertainties the bulk of the stars possesses solar iron abundance, except for star #457, which exhibits an iron abundance that is higher than solar. To within  $3\sigma$  the metallicity distribution looks homogeneous ( $0.4 \pm 0.2$ ), although we believe that more precise estimates of the metallicity would probably reveal some spread, which is expected for a random group of stars.

## 5.2. NGC 2664

For this object we provide two epochs of Echelle spectra. From the analysis of the results of Table 7 we find that one star is a spectroscopic binary (#1826), and due to blending problems we were not able to derive either the spectral types or metallicities of the stars. The remaining three stars do not exhibit significant variations in their radial velocity. Star #2354 is a dwarf, while stars #1890 and #2400 are giants. The studied stars have radial velocities ranging from  $+12 \text{ km s}^{-1}$  to  $+30 \text{ km s}^{-1}$ , thus suggesting that NGC 2664 is not a physical aggregate. The proper

<sup>3</sup> <http://www.astro.lsa.umich.edu/users/hdproj/mosaicinfo/absmag.html>.

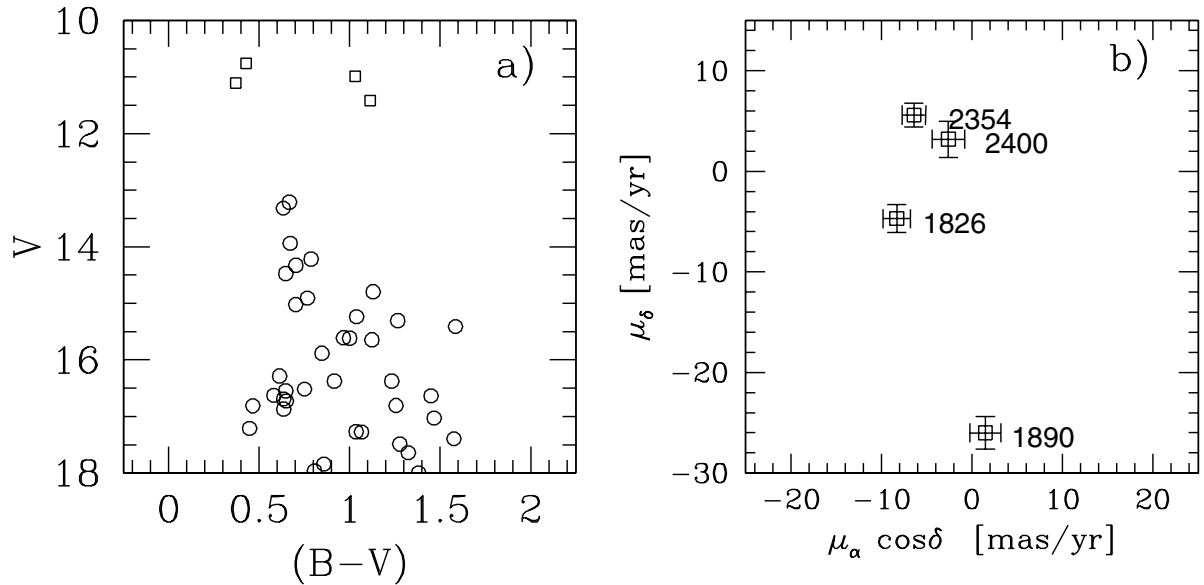


**Fig. 10.** Photometry and proper motions in the region of NGC 2664. **a)** Color–magnitude diagram. Open squares are Tycho 2 stars for which there are both proper motion and radial velocity measurements (see panel b) and Table 7), while filled triangles are stars for which there are only proper motion measurements. **b)** Vector point plot of Tycho 2 proper motions and proper motion errors. Symbols are as in panel a). The identification numbers are from Tycho 2. See text for more details.

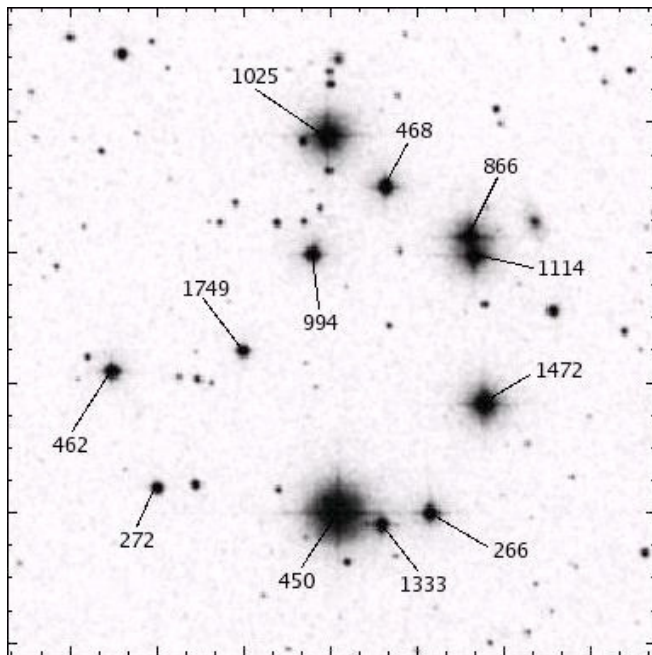


**Fig. 11.** Identification map ( $8'14 \times 8'14$ , taken from DSS-2) for member candidates of Collinder 21 for which there are proper motion measurements from Tycho 2. North is up, East on the left. The labels give the star numbers assigned in the Tycho-2 catalog (in the sense TYC 1759- < ... >). The data for these stars are given in Tables 5 and 8.

motion pair (#2354 and #2400) actually do seem to be a pair, since the radial velocities of the two stars do not differ very much (see Table 7).

Like NGC 5385, we computed spectral type based distances, which are listed in the last column of Table 7. The distance moduli range from 7.70 to 10.41 mag, which implies

distances of 350 to 1207 pc, with slight corrections due to the interstellar reddening, which in the direction of NGC 2664 amounts to 0.02 mag (Schlegel et al. 1998). The four stars that define the group cannot be considered physically bound. Finally, the possible related stars #2354 and #2400 lie too far apart to be considered a physical pair.

In the same table we list estimates of the metal content of three stars, which turns out to be around solar or slightly higher than solar for all the stars within the errors.

### 5.3. Collinder 21

For this object we provide two epochs of medium resolution spectra for all stars except #450, for which we add an Echelle spectrum. Five stars turn out to be giants, and all the others are dwarfs. Though in this case the errors are much larger, from the analysis of the results in Table 8 we confirm that this star (#450) is a binary. Large velocity variations are also shown by the couple #866–#1114 (BD+26 305a,b), which however we are inclined to ascribe to their nature constituting a visual binary. All the other stars show deviating radial velocity, roughly ranging from  $-20 \text{ km s}^{-1}$  to  $+60 \text{ km s}^{-1}$ , thus suggesting that this circlet is not a physical aggregate. The possible proper motion pair (#1472–#272) is not confirmed by radial velocity measurements, and, in addition, these two stars are located in quite different places (see Fig. 11).

Like the previous objects we have derived individual distances for the stars based on spectral classification. The distance moduli range from 3.9 to 10.84 mag, which means distances between 60 and 1470 pc. The reddening in this direction is 0.07 mag (Schlegel et al. 1998), and therefore these estimates do not change significantly because of it. The distance spread is too large to be consistent with Collinder 21 being a physical aggregate.

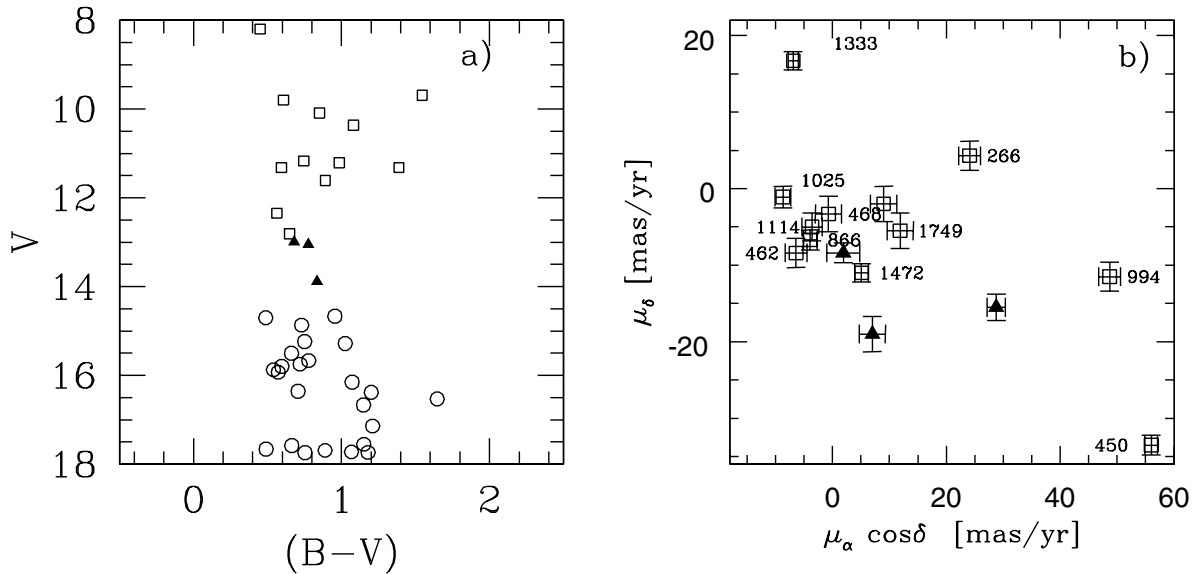


**Fig. 12.** Photometry and proper motions in the region of Collinder 21. **a)** Color–magnitude diagram. Open squares are Tycho 2 stars having both proper motion and radial velocity measurements (see panel b) and Table 8), while filled triangles are stars for which there are only proper motion measurements. **b)** Vector point plot of Tycho 2 proper motions and proper motion errors. Symbols are as in panel a). The identification numbers are from Tycho 2. See text for more details.

Unfortunately, in this case we do not have sufficiently high resolution spectra to derive reasonable estimates of the metal abundance.

## 6. Discussion and conclusions

In this paper we have analysed the possibility that NGC 5285, NGC 2664 and Collinder 21 might be POCRs. Our study however gives a negative answer for all the three.

In fact, star counts and the appearance of the CMDs confirm that we are facing significant stellar overdensities above the general Galactic field.

However, a close scrutiny of the kinematic data (proper motion and radial velocity) provides us with a completely different picture. None of the agglomerates is a physical cluster since they show very different velocity components, and therefore we should consider them simply as chance alignment of unrelated field stars.

We found a number of possible unresolved binary stars or common motion pairs which might deserve further investigation.

The probable binary fraction we found ranges from about 25% in NGC 2664 and NGC 5385 to 18% in Collinder 21, and it is not much different from the typical Galactic disk field binary percentage.

Our findings confirm previous suggestions (Odenkirchen & Soubiran 2002) that an overdensity of stars does not necessarily imply the existence of a physical ensemble, and casts some doubts on the POCR list provided by Bica et al. (2001), which is purely based on star counts. Nevertheless, work is in progress to define a more efficient OCR finding criterion (de la Fuente Marcos, in preparation) and to probe the real nature of other POCR candidates.

*Acknowledgements.* The entire Asiago technical staff is deeply acknowledged for the kind night assistance over the whole duration of this project. G.C. thanks Brian A. Skiff for providing continuous and very useful comments. This study made use of Simbad and WEBDA.

## References

- Bassino, L. P., Waldhausen, N., & Martínez, R. E. 2000, *A&A*, 355, 138
- Baume, G., Villanova, S., & Carraro, G. 2003, *A&A*, 407, 527
- Baumgardt, H. 1998, *A&A*, 340, 402
- Bica, E., Santiago, B. X., Dutra, C. M., et al. 2001, *A&A*, 366, 827
- Carraro, G. 2000, *A&A*, 357, 145
- Carraro, G. 2002, *A&A*, 385, 471
- Carraro, G., Ng, Y. K., & Portinari, L. 1998, *MNRAS*, 246, 1045
- Carraro, G., Bresolin, F., Villanova, S., et al. 2004, *AJ*, in press [arXiv:astro-ph/0406679]
- de la Fuente Marcos, R. 1997, *A&A*, 322, 764
- de la Fuente Marcos, R. 1998, *A&A*, 333, L27
- Desidera, S., Fantinel, D., & Giro, E. 2001, *AFOSC USER MANUAL*
- Dias, W. S., Alessi, B. S., Moitinho, A., & Lepine, J. R. D. 2002, *A&A*, 389, 871
- Halbwach, J. L., Mayor, M., Udry, S., & Arenou, F. 2003, *A&A*, 397, 159
- Høg, E., Fabricius, C., Makarov, V. V., et al. 2000, *A&A*, 355, L27
- Landolt, A. U. 1992, *AJ*, 104, 340
- Monet, D. G., Levine, S. E., Casian, B., et al. 2003, *AJ*, 125, 984
- Odenkirchen, M., & Soubiran, C. 2002, *A&A*, 383, 163
- Patat, F., & Carraro, G. 2001, *MNRAS*, 325, 1591
- Pavani, D. B., Bica, E., Dutra, C. M., et al. 2001, *A&A*, 374, 554
- Schlegel, D. J., Finkbeiner, D. P., & Davis, M. 1998, *ApJ*, 500, 525
- Villanova, S. 2003a, Master Thesis, Padova University
- Villanova, S., Carraro, G., & de la Fuente Marcos, R. 2003b, in *Milky Way Surveys: Structure and Evolution of our Galaxy*, Proc. of the 5th Boston University Astrophysics Conference, in press
- Villanova, S., Baume, G., Carraro, G., & Geminale, A. 2004, *A&A*, 419, 149
- Zacharias, N., Urban, S. E., Zacharias, M. I., et al. 2003, *AJ*, in preparation